Construction and Building Materials 133 (2017) 171–181

Contents lists available at ScienceDirect

Construction and Building Materials

journal homepage: www.elsevier.com/locate/conbuildmat

Durability study on engineered cementitious composites (ECC) under sulfate and chloride environment

Hezhi Liu [a,b,c], Qian Zhang [d], Victor Li [e], Huaizhi Su [a,b,c,*], Chongshi Gu [a,b,c,*]

[a] State Key Laboratory of Hydrology-Water Resources and Hydraulic Engineering, Hohai University, Nanjing 210098, China
[b] College of Water Conservancy and Hydropower Engineering, Hohai University, Nanjing 210098, China
[c] National Engineering Research Center of Water Resources Efficient Utilization and Engineering Safety, Hohai University, Nanjing 210098, China
[d] Department of Civil and Environmental Engineering, University of Louisiana at Lafayette, United States
[e] Department of Civil and Environmental Engineering, University of Michigan, Ann Arbor, MI, United States

HIGHLIGHTS

- ECC remains durable after 200 days of exposure to sulfate and sulfate-chloride environment.
- Long-term exposure leads to compressive and tensile strength increase of ECC.
- Long-term exposure leads to slight reduction of tensile strain capacity of ECC.
- Composite level behavior of ECC is a result of changed matrix fracture toughness and fiber/matrix interfacial bond.
- Tensile ductility reduction of ECC is attributed to reduced crack number and width.

ARTICLE INFO

Article history:
Received 17 August 2016
Received in revised form 16 October 2016
Accepted 16 December 2016
Available online 24 December 2016

Keywords:
Engineered cementitious composites (ECC)
Durability
Sulfate
Chloride
Micromechanics
Hydraulic structures

ABSTRACT

The lack of durability of concrete hydraulic structures, especially under sulfate and chloride environment, has become a worldwide problem. The present paper investigated the feasibility of applying ductile engineered cementitious composites (ECC) as an alternative to conventional concrete in hydraulic structures to improve their durability performance. Specifically, the durability of ECC under sulfate and combined sulfate-chloride conditions were studied. Compressive and tensile behavior of ECC after long-term exposure to Na_2SO_4 and Na_2SO_4 + NaCl solutions was experimentally characterized. Subsequently, micromechanical study was adopted to investigate the microscopic mechanisms underlying the composite level behavior of ECC under those aggressive environments. The research findings demonstrated that ECC remains durable and maintains its high mechanical performance even after 200 days of exposure to concentrated sulfate and combined sulfate-chloride environments. In addition, the micromechanics-based study quantitatively characterized the influence of sulfate and sulfate-chloride solutions on the micromechanical parameters including matrix fracture toughness and fiber/matrix interfacial bond, providing insights into the underlying mechanisms of the composite level behavior of ECC under those environments.

1. Introduction

The durability performance of concrete hydraulic structures in field conditions are often called into question. Most hydraulic structures are designed for a service life of 50 to 100 years depending on their specific application [1]. However, poor durability performance of concrete material often causes deterioration of structures even before their intended service life is reached [2]. For example, the Gutianxi II hydropower station in China faced severe challenges from concrete aging, curtain grouting failure and other problems associated with deterioration only after operation for 30 years, and about four million dollars were spent on maintaining and repairing the structure [3]. Similarly, unsatisfactory performance of aging hydraulic structures also troubles the United States. According to the 2013 report card published by American Society of Civil Engineers (ASCE) [4], the average age of dams in the United States is 52 years. The overall number of high-hazard dams reached nearly 14,000 in 2012 and the number

* Corresponding authors at: State Key Laboratory of Hydrology-Water Resources and Hydraulic Engineering, Hohai University, Nanjing 210098, China.
E-mail addresses: su_huaizhi@hhu.edu.cn (H. Su), csgu@hhu.edu.cn (C. Gu).

http://dx.doi.org/10.1016/j.conbuildmat.2016.12.074
0950-0618/

continues to grow. The required investment for repairing these aging and high-hazard dams is estimated to be up to 21 billion dollars. A worldwide engineering challenge to enhance the durability of hydraulic structures and to lower the maintenance cost has emerged.

In field conditions, the most common cause of insufficient durability of hydraulic structures is the development of cracks within concrete [5,6]. For concrete dams, various causes including mechanical loading, chemical attack, thermal contraction, shrinkage, and foundation settlement can result in concrete cracking [7]. It is generally agreed that cracking in concrete accelerates deterioration by providing easy access for aggressive ions (e.g. sulfate and chloride ions) to get into the interior of the structure [8]. Based on previous study [8,9], the influence of cracks on the corrosion process is negligible when the cracks are relatively narrow; however, the corrosion rate increases significantly when cracks exceed 100 μm in width. Hence, the crack width must be carefully controlled to achieve desirable durability performance of concrete hydraulic structures.

Crack width control, however, is considered a significant challenge for conventional concrete. Great efforts have been made to control crack initiation and propagation within concrete, such as careful selection and proportioning of material, temperature control during construction and using steel reinforcement [10–12]. However, due to the inherent brittleness of concrete, under mechanical and environmental loadings, cracking is almost inevitable [13]. In addition, it is generally recognized that crack width in concrete is difficult to control reliably. Therefore, a material with intrinsic and consistent crack width control capability is highly desirable.

The feasibility of using Engineered Cementitious Composites (ECC) to control crack width and enhance structural durability has been demonstrated in a number of studies [14–17]. ECC is a family of high performance fiber-reinforced cementitious composites featuring high tensile ductility and tight crack width. Under tensile load, ECC exhibits a pseudo strain-hardening behavior by developing multiple micro-cracks. The tensile strain capacity of ECC reaches 3–5% (with less than 2% fiber content by volume), which is 300–500 times that of normal concrete [16–18]. More importantly, the micro-cracks are typically below 60 μm wide. According to previous studies, the tight crack width of ECC is beneficial for preventing initiation of deterioration and slowing down the deterioration rate, leading to extended service life and enhanced serviceability of hydraulic structures.

The durability of ECC under combined mechanical loading and various environmental loadings has been extensively investigated in the past decades. Sahmaran et al. [19] and Li and Li [13] reported that ECC remains durable and exhibits robust high tensile ductility under chloride environment. Özbay et al. [20] investigated the durability of ECC (containing high volumes of slag) subjected to sulfate attack and freeze-thaw cycles. The experimental results indicate that the ductility of ECC specimens decreases after 300 freeze-thaw cycles both in water and Na_2SO_4 solution. In contrast, Lepech and Li [21] found no deterioration of ECC (containing fly ash) when exposed to freeze-thaw cycles. In addition, the durability of ECC under hot and humid environment [22], natural environment [23] and highly alkaline environment [24] were also experimentally studied and demonstrated to be much higher than that of conventional concrete. These prior research show promise in using ECC to improve the long-term durability performance of concrete structures including hydraulic structures.

Among all durability related issues, sulfate attack is considered one of the most critical environmental deterioration mechanisms affecting the durability of concrete hydraulic structures [25]. When in contact with sulfate solution, the chemical reactions between sulfate ions and cement hydration products form expansive compound, causing cracking of concrete. Cracks in concrete allows the sulfate ions to penetrate into the interior of the structure, further accelerating the deterioration. As a result, hydraulic structures serving in sulfate rich environment like Northwest China could fail in less than 5 years, which leads to huge economic loss and social impacts [26,27].

Most previous researches on concrete (and ECC) durability only considered a single deterioration mechanism (such as sulfate attack) which is inconsistent with service condition. In reality, concrete structures may be exposed to combined environmental loadings (such as combined sulfate and chloride attack). This is particularly true for Northwest China where more than 1000 salt lakes are located and also in most marine environments. Under those environments, the durability of hydraulic structures is greatly challenged due to the combined sulfate and chloride attack. Several studies have already pointed out that there exists a clear interaction between the two phenomena [28,29]. Therefore, to fully evaluate the potential of applying ECC in hydraulic structures, it is important to consider the coupled effect of sulfate and chloride attack on the durability of ECC. However, no research on the performance of ECC under this aggressive environment has been conducted so far.

Unlike conventional concrete, ECC is designed based on micromechanics. Micromechanics establishes the linkage between composite level properties (e.g. tensile strength, tensile ductility, and crack widths) and properties at microscale (e.g. matrix toughness and fiber/matrix interfacial bond). Utilizing micromechanics and by investigating the micromechanical properties of ECC, the deterioration mechanisms of ECC composite under sulfate and chloride attack can be revealed.

The objective of the present research is to fully evaluate the durability performance of ECC subjected to sulfate-chloride environment, and to understand the underlying mechanisms of its deterioration under such conditions. For this purpose, the mechanical performance of ECC under sulfate and sulfate-chloride attack were experimentally investigated. Specifically, compressive and tensile properties of ECC after long-term exposure (up to 200 days) were used to evaluate the durability of ECC under such conditions. In addition, micromechanical studies including matrix toughness tests and single-fiber pull-out tests were conducted to fully understand the influence of sulfate and sulfate-chloride attack on ECC material. The research findings here are expected to provide useful data and guidelines for future design and application of ECC in surface repair of hydraulic structures to improve their shielding performance.

2. Experiment procedures

2.1. Materials and mix proportions

A regular ECC mix as found in the literature [30] was used in this study. The constituent materials for this ECC mixture are Type I Portland cement, fine silica sand, class F fly ash, water, high range water reducing agent (HRWRA), and poly-vinyl-alcohol (PVA) fibers. The detailed mix proportion is given in Table 1. The PVA fiber used here has an average diameter of 39 μm and length of 12 mm. The tensile strength and maximum elongation of the fiber are 1600 MPa and 6.0%, respectively. In addition, the surface of the fibers is coated with 1.2% (by weight) proprietary hydrophobic agent to modify the interaction between the fiber and cement matrix for better performance. Mortar specimens adopted from previous study [19] were also prepared as a control to compare with ECC. The mortar mix consists of Type I Portland cement, water and natural river sands. The detailed mix proportion is also shown in Table 1.

Table 1
Mix proportions of ECC and Mortar.

Material	Cement	Aggregates	Fly ash	Water	HRWRA	Fiber
ECC	393	457 (silica sand)	865	311	5	26
Mortar	614	1534 (river sand)	–	215	–	–

2.2. Durability test procedures

A typical ECC mixing procedure [31] was followed to prepare all ECC mixtures. After mixing, fresh ECC were cast into cube specimens measuring 50.8 × 50.8 × 50.8 mm for compression tests, and dogbone-shaped specimens (dimensions as shown in Fig. 1) for uniaxial tension tests. Cube mortar specimens with the same aforementioned size were also prepared for control purpose. All specimens were demolded after 24 h. Afterwards, all cube specimens were covered with wet paper towel and stored in a plastic bag at a room temperature of 23 ± 3 °C until the age of 28 days. Dogbone specimens were directly cured in laboratory air at a temperature of 23 ± 3 °C until 28 days prior to being exposed to sulfate-chloride environments.

In order to investigate the durability of ECC under sulfate and chloride conditions, the following aggressive solutions suggested by former studies [19,20] were prepared:

(1) 5% (by mass) Na_2SO_4 solution.
(2) 5% (by mass) Na_2SO_4 + 3% (by mass) NaCl solution.

At the age of 28 days, cube specimens (ECC and mortar) were put into and kept in the above solutions for 30, 60, 90, 120, 200 and 420 days under laboratory condition, while dogbone specimens were kept for 30, 60, 90, 120 and 200 days. Meanwhile, control cube and dogbone specimens were immersed in water for the same period of time. A set of three specimens was tested for each mixture/exposure condition.

After environmental exposure, the specimens were air-dried for 24 h and tested for their compressive and tensile properties. Compression tests on ECC and mortar specimens were conducted using a compression test system at a loading rate of 1300 ± 300 N/s in accordance with ASTM C109 [32]. Uniaxial tension tests were conducted in accordance to the recommendations for direct tension testing of High Performance Fiber Reinforced Cementitious Composites by the Japan Society of Civil Engineers (JSCE) [33]. Uniaxial tensile loading was imposed on the specimens under displacement control at a rate of 0.5 mm/min. Two external linear variable differential transducers (LVDTs) were attached on each side of the specimen, with a gage length of approximately 80 mm, to measure the tensile strain. The tensile test setup is shown in Fig. 2.

2.3. Micromechanical investigation

The core of the micromechanics-based ECC theory are the two conditions that must be met for the composite to show strain-hardening behavior under tension, which can be expressed in energy and strength terms, as shown in Eqs. (1) and (2):

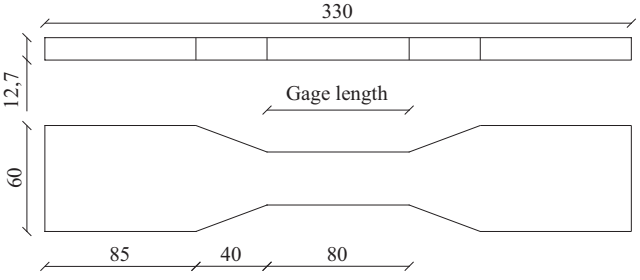

Fig. 1. Dimensions of dogbone specimens for uniaxial tension test (unit: mm).

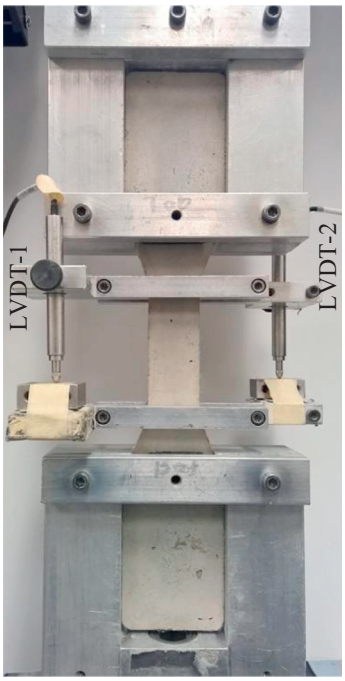

Fig. 2. Uniaxial tensile test setup.

$$\text{Energy-based criterion}: J_b' \equiv \sigma_0\delta_0 - \int_0^{\delta_0}\sigma(\delta)d\delta \geqslant J_{tip} \approx \frac{K_m^2}{E_m} \quad (1)$$

$$\text{Strength-based criterion}: \min(\sigma_0) > \sigma_c \quad (2)$$

where J_b' is the fiber bridging complementary energy; J_{tip} is the fracture energy of the matrix; σ_0 and δ_0 are the maximum bridging stress of the crack plane and corresponding crack opening; $\sigma(\delta)$ is the fiber bridging stress versus crack opening relationship of the crack plane; σ_c is the cracking strength of the matrix; K_m and E_m are matrix fracture toughness and matrix Young's modulus, respectively.

Energy based criterion describes the energy balance during crack extension. Eq. (1) requires that the complementary energy J_b' (associated with fiber/matrix interfacial bond) to be greater than the fracture energy of the matrix J_{tip} (associated with matrix toughness), as illustrated in Fig. 3. This guarantees the formation of flat cracks under tension instead of the normal Griffith cracks [34–36], and formation of flat cracks allows more cracks with tight crack width to form without extensive fiber rupture/pullout [15,16]. Strength based criterion requires the maximum fiber bridging capacity to be higher than the matrix cracking strength. It is obvious that the strength based criterion also need to be met to allow formation of more than one cracks. Therefore, satisfaction of both criteria is necessary to achieve strain-hardening behavior of ECC. Otherwise, a single localized fracture, and normal tension-softening behavior as in the case of FRC will result.

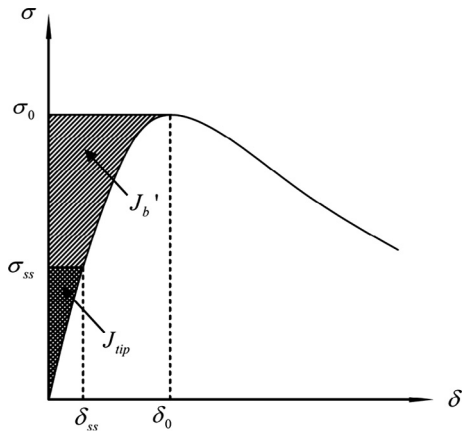

Fig. 3. Typical fiber bridging stress versus crack opening $\sigma(\delta)$ curve [14]. Hatched area represents maximum complementary energy J_b'. Cross area represents the fracture energy of matrix J_{tip}.

Based on above strain-hardening criteria, two pseudo strain-hardening indices as defined in Eqs. (3) and (4) can be used to predict the tensile performance of ECC composites based on micromechanical properties.

$$PSH_E = \frac{J_b'}{J_{tip}} \tag{3}$$

$$PSH_S = \frac{\min(\sigma_0)}{\sigma_c} = \frac{\sigma_t}{\sigma_c} \tag{4}$$

where σ_t is the (ultimate) tensile strength of ECC composite. As previously discussed, both indices need to be greater than 1 for ECC to achieve strain-hardening behavior and high tensile ductility. Considering variability in material properties, in practice, PSH_E and PSH_S need to be greater than 3 and 1.2, respectively to achieve robust strain-hardening behavior [37]. In fact, PSH_s index typically does not govern for PVA-ECC, while PSH_E index is considered as the dominant factor that determines the tensile behavior of ECC. Therefore, only PSH_E index was considered and discussed in this study.

To quantitatively assess the influence of sulfate and sulfate-chloride attack on micromechanical properties of ECC, matrix fracture toughness test and single fiber pullout test were conducted.

Matrix fracture toughness test (in accordance with ASTM E399 [38]) uses a three-point bend loading on notched beam specimens made of ECC matrix (without fibers). The detailed configuration of the test is shown in Fig. 4. The beam specimens measure 305 mm long, 76 mm wide and 38 mm deep and were cast from ECC mixtures without fibers. The specimens were cured in laboratory air under 23 ± 3 °C and 20 ± 5% RH for 28 days before exposed to the sulfate and sulfate-chloride solutions for 30, 60, 90 and 200 days. After designated environmental exposure, the specimens were air-dried for 24 h and tested for matrix fracture toughness. Prior to the test, a thin notch (0.6 mm thick) was made on the tension face of the beam specimen at mid-span (as shown in Fig. 4) to initiate the fracture. The notch depth to beam height ratio is 0.4 as recommended by ASTM E399. Four specimens were tested for each case.

Based on the measured fracture load during the test, the matrix fracture toughness K_m was determined. Assuming the Young's modulus of the matrix is the same as that of the composite (since the fiber volume fraction is low), using the modulus of ECC composite calculated from the tensile stress-strain relationship, J_{tip} was calculated following the right hand side expression of Eq. (1).

In order to obtain J_b', single fiber pullout tests were conducted to determine the interfacial parameters including chemical bond strength G_d, frictional bond strength τ_0 and slip hardening coefficient β. During the test, individual fibers with embedment lengths of approximately 1 mm were pulled out of small ECC mortar prisms, as shown in Fig. 5. The details of specimen preparation and test configuration can be found in [39]. The preparation of single fiber specimens followed the same curing and conditioning procedure as for the beam specimens. Considering that single fiber

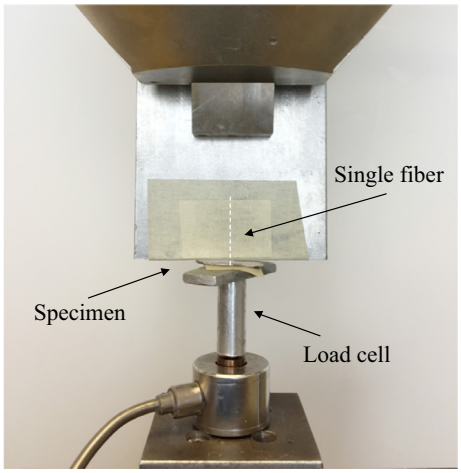

Fig. 5. Single-fiber pullout test setup.

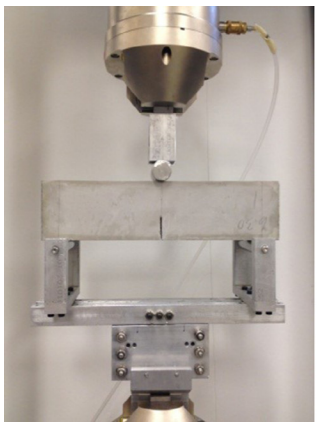

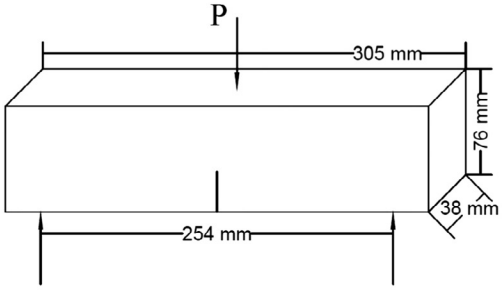

Fig. 4. Matrix fracture toughness test setup.

test, by nature exhibits large scatter in the data, twenty specimens were prepared and tested for each case. Once the single fiber pull-out behavior was characterized, by considering the average pull-out behavior of all the fibers on a cross section, the fiber bridging stress-crack opening ($\sigma(\delta)$) relationship can be derived [14]. The complementary energy J_b' was then calculated from $\sigma(\delta)$ relationship. Together with the matrix fracture toughness from the K_m measurement, PSH_E index was determined.

3. Experimental results and discussion

3.1. Compressive behavior

The measured compressive strength of ECC and mortar specimens exposed to Na_2SO_4 solution, Na_2SO_4 + NaCl solution, and water is shown in Fig. 6. As can be seen, the compressive strength of specimens cured in water showed a notable increasing trend at the beginning stage up to 60 days for ECC specimens and 30 days for mortar specimens, respectively. Then the rate of strength increase slowed down and became stabilized. The strength increase is attributed to the continuous hydration of cement and the pozzolanic reaction of fly ash. Similar trend was observed for ECC specimens that were exposed to Na_2SO_4 solution and Na_2SO_4 + NaCl solution: the compressive strength experienced a sharp increase in the initial stage, and it was followed by a relatively sluggish rise until the end of exposure. For those specimens, in addition to continuous cement hydration and pozzolanic reaction (only in ECC), sulfate ions were diffused into the pores within the mortar specimen and reacted with the cement hydration products to form ettringite and gypsum, which may also contribute to the strength gain.

For mortar specimens subjected to Na_2SO_4 solution and Na_2SO_4 + NaCl solution, the strength continues to increase up to 120 days and to 200 days respectively, after which significant drops were observed for specimens under both exposure conditions. Specifically, the compressive strength decreased from 71 MPa and 73 MPa to around 56 MPa respectively for specimens exposed to Na_2SO_4 solution and Na_2SO_4 + NaCl solution. This was also accompanied by surface cracks after 420 days (Figs. 7 and 8). Mortar specimen at 28 days was shown in Fig. 9. As can be seen, no surface cracks were observed before exposure. Therefore, the surface cracking is likely due to internal pressure caused by the continued formation of expansive ettringite even when the pores were completely filled, when sulfate ions reacted with cement hydrates. When such pressure exceeded the mortar's tensile strength, cracks formed. However, for ECC specimens in Na_2SO_4 solution and Na_2SO_4 + NaCl solution, neither compressive strength reduction nor surface cracking (as shown in Figs. 7 and 8) was observed. This could be attributed to the fact that ECC has much higher tensile performance that delayed the cracking. The delay of surface cracking kept diffusivity of sulfate ions low and prevented accelerated deterioration. In addition, even when ECC eventually cracks, the cracks will be much tighter compared to that of mortar specimens, therefore preventing dramatic increase of the diffusivity of aggressive ions and keeping the deterioration slow. As a result, ECC provides better sulfate resistance than normal mortar specimens, which is highly desirable for hydraulic structures in sulfate-rich environments.

With regards to the effect of chlorides on sulfate attack, Fig. 6 clearly shows that the compressive strength of all ECC specimens subjected to Na_2SO_4 + NaCl solution is lower than that of the same-age specimens exposed to Na_2SO_4 solution during the whole

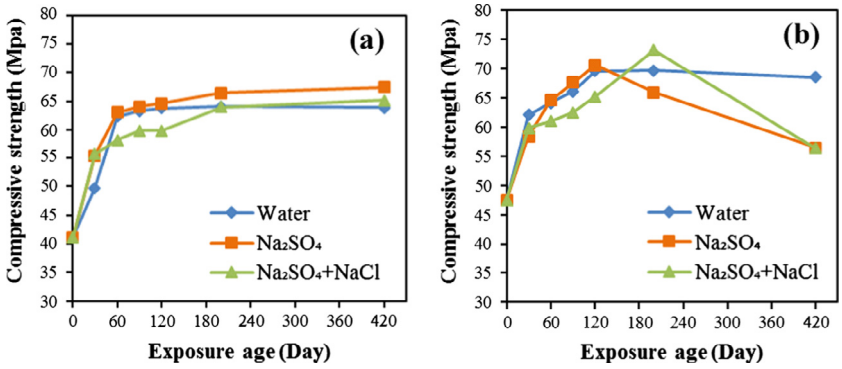

Fig. 6. Compressive strength of (a) ECC and (b) mortar specimens subjected to different environmental exposures.

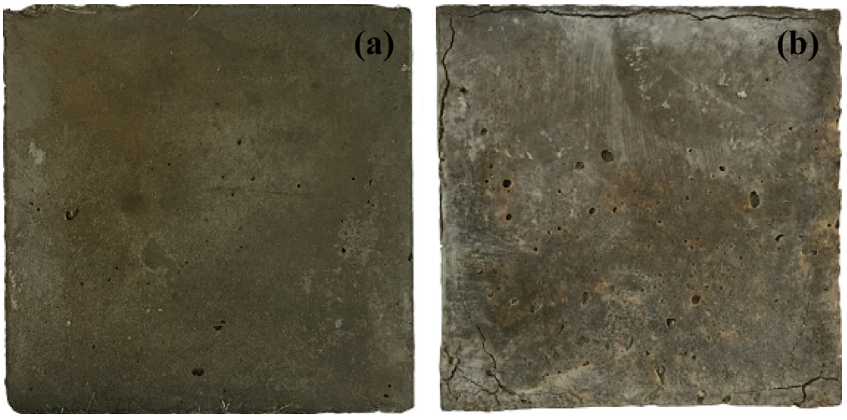

Fig. 7. (a) ECC and (b) mortar specimen after 420-day Na_2SO_4 exposure.

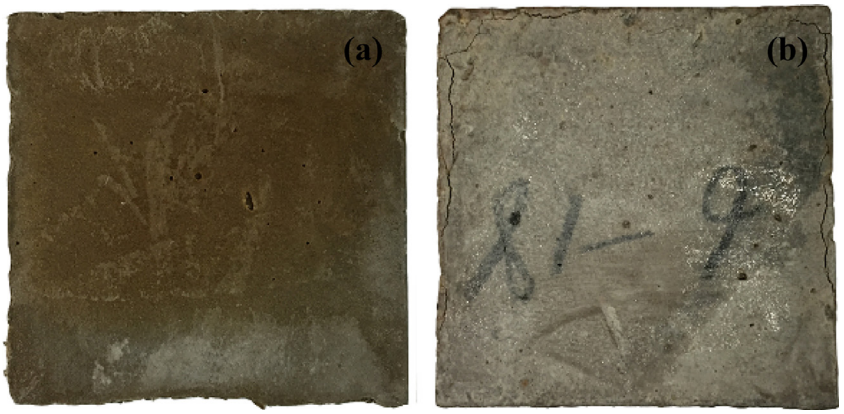

Fig. 8. (a) ECC and (b) mortar specimen after 420-day Na_2SO_4 + NaCl exposure.

Fig. 9. Mortar specimen before exposure to aggressive solutions at 28 days.

exposure period. For mortar specimens, a similar trend was observed at the initial 120 days, after which the compressive strength of specimens in Na_2SO_4 solution tended to decrease, while specimens in Na_2SO_4 + NaCl solution maintained the upward trend until 200 days. This indicates that the presence of chloride ions slowed down the sulfate attack process and therefore the strength increasing (and possible later decreasing) trend was shifted. According to prior studies [28,29,40–42], this is mainly attributed to the following reasons: (1) The sulfate diffusion rate is lower for Na_2SO_4 + NaCl composite solution than that for the Na_2SO_4 solution. (2) The rate of chloride diffusion is much higher than that of sulfate diffusion, therefore C_3A firstly reacts with chloride ions and forms calcium chloroaluminate hydrate (Friedel's salt), and the quantity of C_3A available for the sulfate ions to react with is consequently reduced. (3) The solubility of ettringite in chloride solution is three times greater than that in water, thereby resulting in a lower ettringite precipitation. However, experiments that consider longer exposure time are needed in the future to further characterize the long-term performance of ECC and mortar specimens in Na_2SO_4 + NaCl solution.

3.2. Tensile behavior

Table 2 presents the measured (ultimate) tensile strength, strain capacity and the average crack width of ECC specimens subjected to different exposure conditions. The average crack width presented in the table was obtained based on the method described in [43]. Typical tensile stress-strain curves of ECC specimens under different exposure conditions are also shown in Fig. 10.

From the test results, it can be seen that the tensile strength of ECC specimens exposed to water, Na_2SO_4 solution and Na_2SO_4 + NaCl solution all witnessed an increase over time. Specifically, the average tensile strength of ECC specimens at 28 days is 5.02 MPa. After 200 days' exposure to Na_2SO_4 and Na_2SO_4 + NaCl solutions, the value has risen to 6.29 MPa and 6.22 MPa respectively. For specimens kept in water, relatively smaller increase

Table 2
Tensile properties of ECC under different exposure conditions.

Exposure condition	Exposure time (days)	Tensile strength (MPa)	Strain capacity (%)	Average crack width (μm)
	0	5.02 ± 0.26	4.20 ± 0.14	55
Water	30	5.65 ± 0.27	2.93 ± 0.72	52
	60	5.81 ± 0.10	2.53 ± 0.39	51
	90	5.53 ± 0.19	2.36 ± 0.25	46
	200	5.62 ± 0.02	2.65 ± 0.79	49
Na_2SO_4	30	5.52 ± 0.20	2.14 ± 0.03	49
	60	5.80 ± 0.31	2.69 ± 0.09	48
	90	6.24 ± 0.09	2.21 ± 0.28	50
	200	6.29 ± 0.08	2.14 ± 0.12	47
Na_2SO_4 + NaCl	30	5.84 ± 0.21	3.30 ± 0.23	49
	60	5.61 ± 0.09	2.11 ± 0.01	51
	90	6.45 ± 0.18	3.11 ± 0.17	48
	200	6.22 ± 0.12	2.12 ± 0.23	50

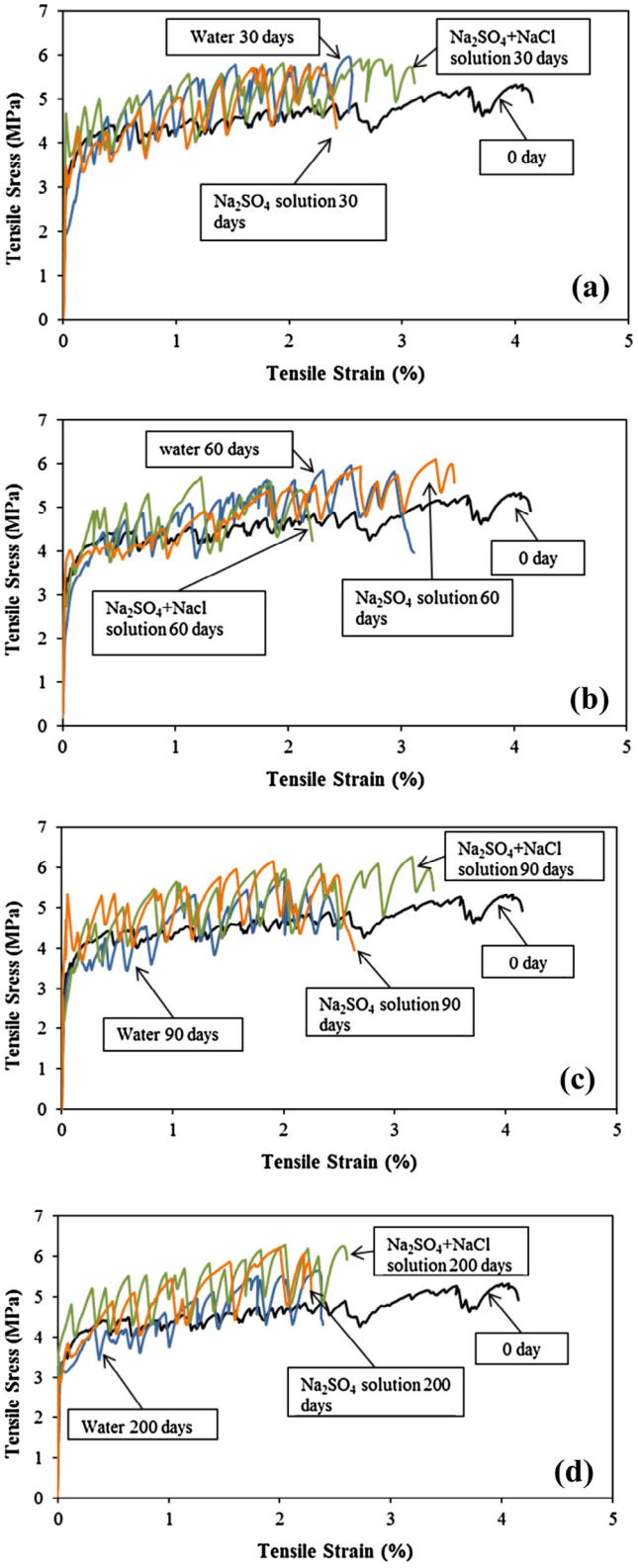

Fig. 10. Typical tensile stress-strain relationship of ECC specimens under different exposure conditions for (a) 30 days, (b) 60 days, (c) 90 days and (d) 200 days.

(from 5.02 MPa to 5.62 MPa) was observed after 200 days of exposure. This is similar to the trend of compressive strength. The strength gain is again associated with continuous hydration of cement, pozzolanic reaction of fly ash and the reaction between sulfate and hydration products. These reactions could densify the interface between fibers and matrix, resulting in higher fiber bridging strength.

With regards to tensile strain capacity, a slight declining tendency with exposure age was noticed for all specimens, especially from 0 to 30 days. After 30 days' exposure, the strain capacity became stabilized and all remained above 2%. It should be noted that despite the observed decreasing trends, the tensile ductility of ECC after environmental exposure is still two orders of magnitude higher than that of normal concrete.

The high tensile ductility of ECC is a result of the multiple-cracking and strain-hardening behavior, which was well preserved after 30, 60, 90 and 200 days of exposure to both water and aggressive solutions. However, the average crack width dropped from 55 μm to 49 μm (water exposure), 47 μm (Na_2SO_4 solution exposure) and 50 μm (Na_2SO_4 + NaCl solution exposure) respectively after 200 days' exposure. The drop in crack width is associated with change of fiber/matrix interfacial properties, which will be discussed in details in Section 3.3. Such decrease of average crack width, although led to a slight reduction in tensile ductility, is helpful for limiting the diffusion of sulfate and chloride ions into the interior of the structures, slowing down the deterioration, and enhancing the durability of hydraulic structures.

3.3. Micromechanical investigation

The composite behavior, especially tensile behavior of ECC under sulfate and sulfate-chloride environments can be further understood by looking into their micromechanical properties. The measured micromechanical parameters (matrix fracture toughness K_m, chemical bond G_d, frictional bond τ_0 and slip hardening coefficient β) as a function of exposure time were plotted in Fig. 11.

The matrix fracture toughness of ECC specimens exposed to Na_2SO_4 and Na_2SO_4 + NaCl solutions all showed increasing trends. For ECC specimens subjected to Na_2SO_4 solution, the matrix fracture toughness increased notably during the first 30 days followed by a relatively stable growth until the end of the test. The rise of matrix toughness is most likely due to the continuous hydration of cement, the pozzolanic reaction of fly ash and the formation of ettringite and gypsum in sulfate environments that densifies the matrix. For specimens that were immersed in Na_2SO_4 + NaCl solution, a slightly more gradual increasing trend and slight lower matrix fracture toughness were observed, as the presence of chloride ions might have affected the formation of ettringite and gypsum.

Regarding the fiber/matrix interfacial properties, despite the large scatter of the single-fiber pullout test results, a significant reduction in chemical bond G_d, and a notable increase in frictional bond τ_0 were observed as shown in Fig. 11. According to previous studies [44,45], chemical bond G_d is governed by the metal cation concentration at the interface, in particular Al^{3+} and Ca^{2+}; frictional bond τ_0 is controlled by the microstructure of interfacial transition zone. In the presence of sulfate and chloride ions, the concentration of Al^{3+} and Ca^{2+} tended to decrease due to the reaction that forms ettringite and gypsum. Besides, the existence of chloride ions could increase the leaching of Ca^{2+} [46,47]. Therefore, chemical bond G_d showed a decreasing trend. While for frictional bond τ_0, the densification of the fiber/matrix interfacial transition zone due to the continuous formation of hydration product, ettringite and gypsum mainly contributed to the increasing trend. With regard to the slip hardening coefficient β, no significant change was observed.

It should also be noted that all the micromechanical parameters as presented in Fig. 11 showed sharper changes during the first 30 days and became stabilized later on. This is also consistent with

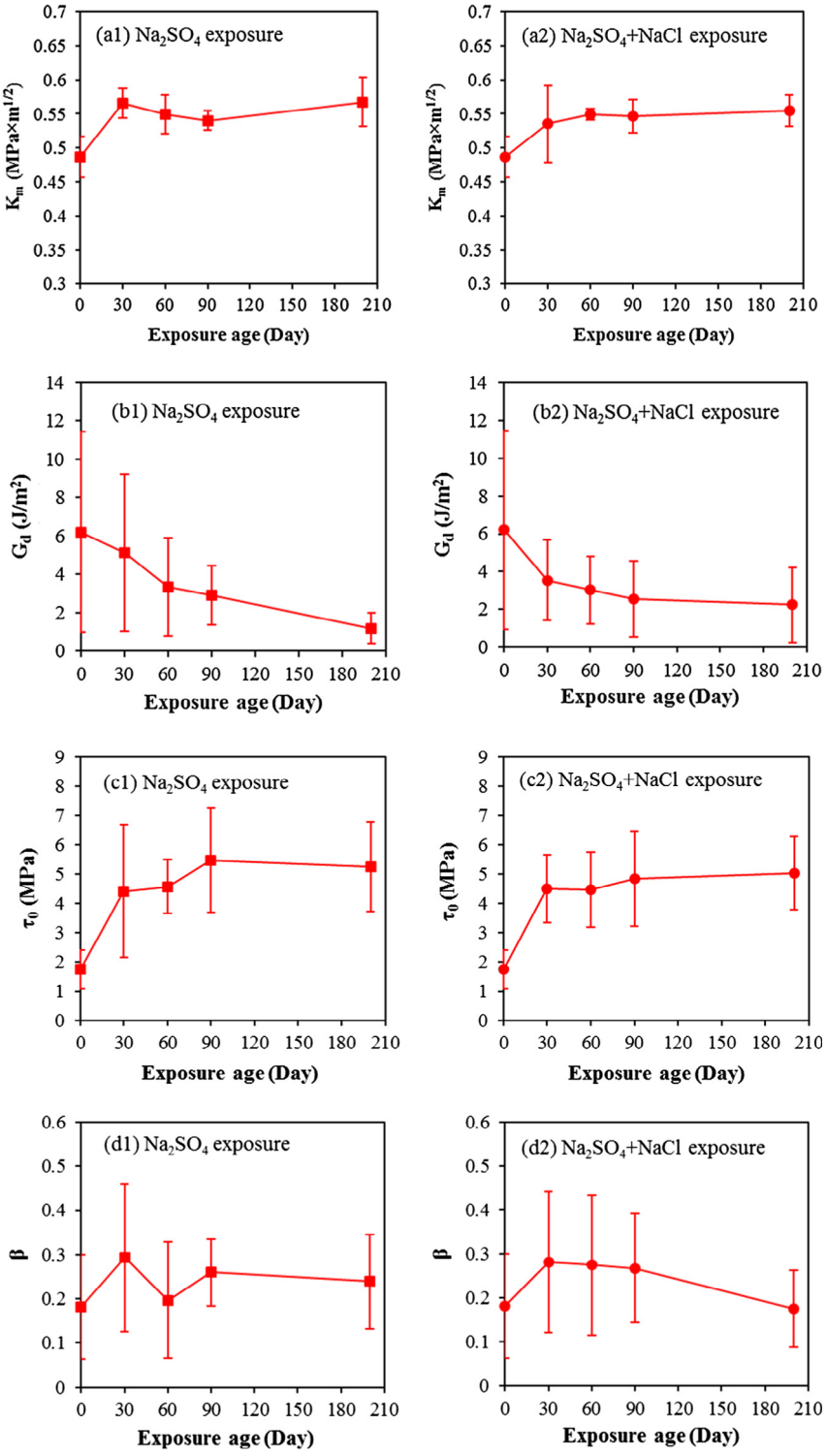

Fig. 11. Influence of Na_2SO_4 and Na_2SO_4 + NaCl exposure on ECC micromechanical parameters: (a) matrix fracture toughness K_m, (b) chemical bond G_d, (c) frictional bond τ_0 and (d) slip hardening coefficient β.

the composite level compressive/tensile behavior. It indicates that the related reactions mainly happened during the initial exposure and slowed down afterwards.

The change of micromechanical parameters directly affected the fiber bridging $\sigma(\delta)$ curves, thereby altered the tensile behavior of ECC composite. Based on the calculated results, after exposure to Na_2SO_4 and Na_2SO_4 + NaCl solutions, the fiber bridging curves shifted upwards and leftwards. The computed fiber bridging $\sigma(\delta)$ relationships at 28 days and after environmental exposures are plotted in Fig. 12, which clearly show the curve shift.

As can be seen, despite the decreasing chemical bond G_d, the maximum fiber bridging stress increased after environmental exposure due to the increasing frictional bond τ_0. This explains the increase of the tensile strength at composite level. In addition, the curve shifting leftwards also reduced the crack width. This is also consistent with the observed crack width data. The value of

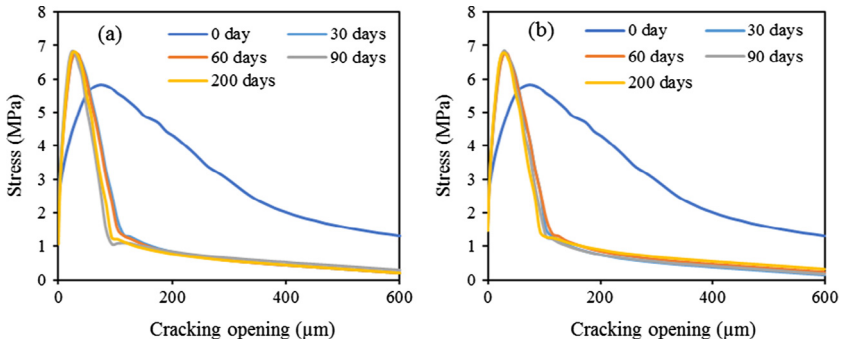

Fig. 12. Calculated $\sigma(\delta)$ curves for specimens before and after 200-day exposure to (a) Na_2SO_4 and (b) Na_2SO_4 + NaCl solution.

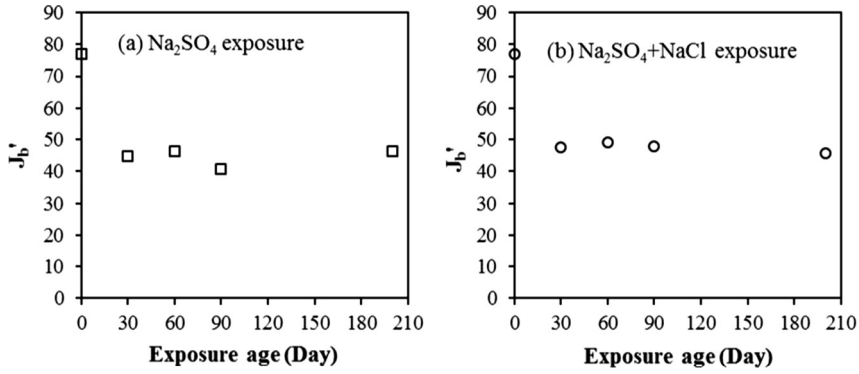

Fig. 13. Influence of (a) Na_2SO_4 and (b) Na_2SO_4 + NaCl exposure on J_b'.

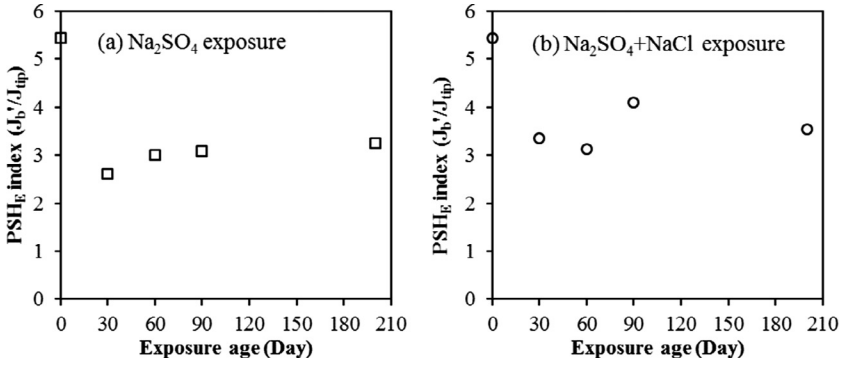

Fig. 14. Influence of (a) Na_2SO_4 and (b) Na_2SO_4 + NaCl exposure on PSH_E index.

the complementary energy J_b' was calculated from the $\sigma(\delta)$ relationship and shown in Fig. 13. From the plot, it is seen that J_b' dropped after the initial exposure to aggressive solutions but remained stable within the remaining exposure period.

The calculated PSH_E index (J_b'/J_{tip}) is shown in Fig. 14. As can be seen, the index dropped from 5.44 (before exposure) to 3.00 (exposure to Na_2SO_4 solution) and 3.12 (exposure to Na_2SO_4 + NaCl solution) after 60 days of exposure, and then the value slightly increased to 3.26 and 3.54 for specimens subjected to 200-day Na_2SO_4 solution and Na_2SO_4 + NaCl solution respectively. The recovery is mainly attributed to the increase of Young's modulus and the associated reduced matrix fracture energy J_{tip}. Throughout the entire environmental exposure, PSH_E index was above 3 at most of the time, which guaranteed saturated and robust multiple cracking behavior. Fig. 15 shows the tested tensile specimens before and after environmental conditioning. As can be seen, even though there is a slightly decrease in crack number after environmental exposure, all specimens showed significant multiple cracking behavior.

Macroscopically, the tensile ductility is governed by both crack width and crack number. Crack number is controlled by the strain-hardening potential as reflected in the PSH_E index. Crack width is essentially determined by the fiber bridging $\sigma(\delta)$ curves. The decrease in tensile strain capacity of ECC after environmental exposure is a combined result of both slightly reduced crack number (caused by reduced PSH_E) in certain exposure cases and reduced crack width. Nevertheless, ECC still showed significant multiple cracking behavior, and reduced crack width is actually considered beneficial for enhancing the durability of ECC in hydraulic structure applications.

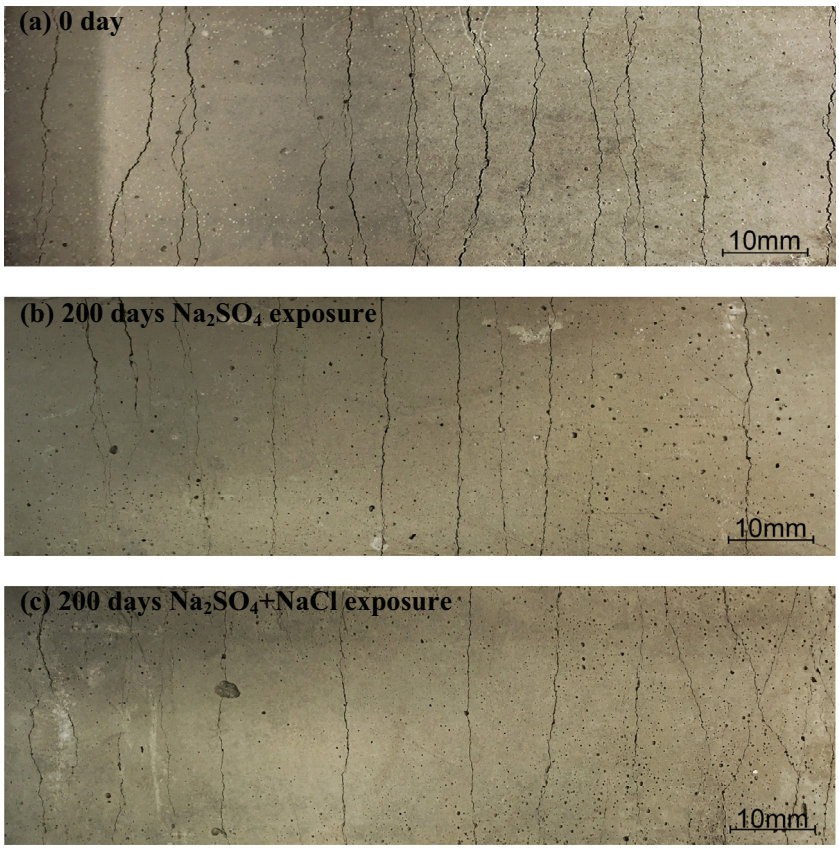

Fig. 15. Multiple cracking behavior of tensile specimens (a) before exposure and after 200-day exposure to (b) Na_2SO_4 and (c) Na_2SO_4 + NaCl solution.

4. Conclusions

This paper experimentally investigated the durability of ECC under sulfate and sulfate-chloride environment. Specific conclusions can be drawn as follows:

(1) ECC remains durable after 420 days of exposure to concentrated sulfate and sulfate-chloride environment. In contrast, notable deterioration was observed for mortar specimens under the same exposure conditions. The research findings demonstrated the feasibility of using ECC to enhance the performance and extend the service life of hydraulic structures under aggressive environments.
(2) Long-term exposure to aggressive (sulfate and sulfate-chloride) solutions leads to increase of compressive strength, tensile strength and a reduction of tensile strain capacity of ECC. Nevertheless, ECC retains multiple cracking and strain-hardening behavior with desirable high tensile ductility above 2% after 200 days of environmental exposure.
(3) The observed composite level behavior of ECC is a result of increased matrix fracture toughness, decreased fiber/matrix interfacial chemical bond and increased interfacial frictional bond upon both sulfate and sulfate-chloride exposures.
(4) The reduction in tensile ductility of ECC after exposure to sulfate and sulfate-chloride conditions is caused by slight decrease of crack number and reduced crack width. Nevertheless, ECC still retain significant multiple cracking and strain-hardening behavior. In addition, the crack width reduction is considered beneficial for long-term durability performance.

It should be noted that the above conclusions were drawn based on the current experimental results up to 420 days of exposure to Na_2SO_4 and Na_2SO_4 + NaCl solutions. Further studies with longer exposure time are needed for better understanding of the long-term performance of ECC under those environments. The findings and micromechanics-based investigation approach of the present study serve as a valuable guideline for future studies. In addition, although the coupled effect of sulfate and chloride attack has been investigated under laboratory condition in this paper, field conditions are more complicated. Future in-situ tests will be of value for a more complete assessment of ECC's potential in hydraulic structure applications.

Acknowledgments

This research was partially funded by National Natural Science Foundation of China (Grant Nos. 51139001, 51479054, 51579083, 41323001), the National Key Research and Development Program of China (Grand No. 2016YFC0401601), the Doctoral Program of Higher Education of China (Grant No. 20130094110010), the Fundamental Research Funds for the Central Universities (Grant No. 2015B25414), China Scholarship Council (CSC) and the China Thousand Talent Program. This research was performed at the University of Michigan, Ann Arbor, while H. Liu served as a visiting scholar.

References

[1] A.J. Schleiss, R.M. Boes, Dams and Reservoirs Under Changing Challenges, CRC Press, 2011.
[2] C. Liu, Z. Wang, Present situation of dam concrete's lifetime in world and existing problems in China, J. Yangtze River Sci. Res. Inst. 17 (1) (2000) 17–20.

[3] L. Xing, G. Nie, Analysis on durability of concrete structure of hydropower stations in China, J. Hydroelectric Eng. 29 (2) (2003) 27–31.
[4] ASCE, 2013 Report Card for America's Infrastructures, 2013.
[5] K. Li, M. Ma, X. Wang, Experimental study of water flow behaviour in narrow fractures of cementitious materials, Cem. Concr. Compos. 33 (10) (2011) 1009–1013.
[6] T.S. Han, P.H. Feenstra, S.L. Billington, Simulation of highly ductile fiber-reinforced cement-based composite components under cyclic loading, ACI Struct. J. 100 (6) (2003) 749–757.
[7] ACI Committee 224, Control of cracking in concrete structures, ACI J. Proc. 69 (12) (1972) 717–753.
[8] M. Tsukamoto, Tightness of fiber concrete, Darmstadt Concr. 5 (1990) 215–225.
[9] V.C. Li, H. Stang, Elevating FRC material ductility to infrastructure durability, in: 6th RILEM Symposium on Fiber-Reinforced Concretes (FRC) – BEFIB 2004, Varenna, Italy, 2004, pp. 171–186.
[10] B.Y. Ding, G.B. Wang, S.P. Huang, Y. Yue, H.P. Zhen, A review on causes of cracking in domestic concrete dams and preventive measures, Water Resour. Hydropower Eng. 25 (4) (1994) 12–18.
[11] Y. Ma, Y. Zhu, Y. Liu, Y. Ning, Feedback study of temperature control and crack prevention of Jiangtanghu pump concrete sluice during construction, Water Power 32 (1) (2006) 33–35.
[12] B.F. Zhu, Current situation and prospect of temperature control and cracking prevention technology for concrete dam, J. Hydraul. Eng. 37 (12) (2006) 1424–1432.
[13] M. Li, V.C. Li, Cracking and healing of engineered cementitious composites under chloride environment, ACI Mater. J. 108 (2011) 333–340.
[14] V.C. Li, Engineered cementitious composites (ECC) - tailored composites through micromechanical modeling, in: N. Banthia, A. Bentur, A. Mufti (Eds.), Fiber Reinforced Concrete: Present and the Future, Canadian Society of Civil Engineers, 1997, pp. 1–38.
[15] V.C. Li, Advances in ECC research, ACI Spec. Publ. Concr. 206 (2002) 373–400.
[16] V.C. Li, On engineered cementitious composites (ECC) – a review of the material and its applications, J. Adv. Concr. Technol. 1 (3) (2003) 215–230.
[17] V.C. Li, Engineered cementitious composites (ECC) – material, structural, and durability performance, Concrete Construction Engineering Handbook, vol. 78, 2008.
[18] V.C. Li, S. Wang, C. Wu, Tensile strain-hardening behavior or polyvinyl alcohol engineered cementitious composite (PVA-ECC), ACI Mater. J. 98 (6) (2001) 483–492.
[19] M. Sahmaran, M. Li, V.C. Li, Transport properties of engineered cementitious composites under chloride exposure, ACI Mater. J. 104 (6) (2007) 604–611.
[20] E. Özbay, O. Karahan, M. Lachemi, K.M. Hossain, C.D. Atis, Dual effectiveness of freezing-thawing and sulfate attack on high-volume slag-incorporated ECC, Composites Part B 45 (1) (2013) 1384–1390.
[21] M. Lepech, V.C. Li, Long term durability performance of engineered cementitious composites, Restor. Build. Monuments 12 (2) (2006) 119–132.
[22] V.C. Li, T. Horikoshi, A. Ogawa, S. Torigoe, T. Saito, Micromechanics-based durability study of polyvinyl alcohol-engineered cementitious composite, ACI Mater. J. 101 (3) (2004) 242–248.
[23] V.C. Li, E.N. Herbert, Self-healing of microcracks in engineered cementitious composites (ECC) under a natural environment, Materials 6 (7) (2013) 2831–2845.
[24] M. Sahmaran, V.C. Li, Durability of mechanically loaded engineered cementitious composites under highly alkaline environments, Cem. Concr. Compos. 30 (2) (2008) 72–81.
[25] R. Charlwood, Predicting the long term behavior and service life of concrete dams, in: Conference on Long Term Behavior of Dams, 2009, pp. 1–11.
[26] T.P. Dolen, G.A. Scott, K.F. von Fay, B. Hamilton, Effects of Concrete Deterioration on Safety of Dams, Dam Safety Office, 2003.
[27] M.T. Bassuoni, M.L. Nehdi, Durability of self-consolidating concrete to sulfate attack under combined cyclic environments and flexural loading, Cem. Concr. Res. 39 (3) (2009) 206–226.
[28] O.S.B. Al-Amoudi, M. Maslehuddin, Y.A.B. Abdul-Al, Role of chloride ions on expansion and strength reduction in plain and blended cements in sulfate environments, Constr. Build. Mater. 9 (1) (1995) 25–33.
[29] Z.Q. Jin, W. Sun, Y.S. Zhang, J.Y. Jiang, J.Z. Lai, Interaction between sulfate and chloride solution attack of concretes with and without fly ash, Cem. Concr. Res. 37 (8) (2007) 1223–1232.
[30] Z. Zhang, S. Qian, H. Ma, Investigating mechanical properties and self-healing behavior of micro-cracked ECC with different volume of fly ash, Constr. Build. Mater. 52 (2) (2014) 17–23.
[31] X. Huang, R. Ranade, V.C. Li, Feasibility study of developing green ECC using iron ore tailings powder as cement replacement, J. Mater. Civil Eng. 25 (7) (2012) 923–931.
[32] Standard test method for compressive strength of hydraulic cement mortars (using 2-in. or [50-mm] cube specimens), ASTM Int. (2016).
[33] JSCE concrete committee, recommendations for design and construction of high performance fiber reinforced cement composites with multiple fine cracks, Jpn. Soc. Civil Eng. (2008).
[34] A.A. Griffith, The phenomena of rupture and flow in solids, Philos. Trans. R. Soc. London Ser. A 221 (1921) 163–198.
[35] V.C. Li, C.K. Leung, Steady-state and multiple cracking of short random fiber composites, J. Eng. Mech. ASCE 118 (11) (1992) 2246–2264.
[36] V.C. Li, H.C. Wu, Conditions for pseudo strain-hardening in fiber reinforced brittle matrix composites, Appl. Mech. Rev. 45 (8) (1992) 390–398.
[37] T. Kanda, Design of Engineered Cementitious Composites for Ductile Seismic Resistant Elements, University of Michigan, 1998.
[38] American Society for Testing and Materials, Standard Test Method for Linear-Elastic Plane-Strain Fracture Toughness KIc of Metallic Materials, ASTM, West Conshohocken, PA, 2013.
[39] C. Redon, V.C. Li, C. Wu, H. Hoshiro, T. Saito, A. Ogawa, Measuring and modifying interface properties of PVA fibers in ECC matrix, J. Mater. Civil Eng. 13 (6) (2001) 399–406.
[40] D.G. Miller, Laboratory investigation of the influence of curing conditions and various admixtures on the life of concrete stored in sulphate solutions as indicated by physical changes, Proc ASTM, 1924, pp. 847–863.
[41] A. Yeginobali, Sulfate resistance of mortars mixed with sea waters, in: Proc 3rd International Conference on Durability of Building Materials and Components, 1984, pp. 55–65.
[42] W. Harrison, Effect of chloride in mix ingredients on sulphate resistance of concrete, Mag. Concr. Res. 42 (152) (1990) 113–126.
[43] H. Liu, Q. Zhang, C. Gu, H. Su, V. Li, Influence of micro-cracking on the permeability of engineered cementitious composites, Cem. Concr. Compos. 72 (2016) 104–113.
[44] S. Wang, V. Li, Engineered cementitious composites with high-volume fly ash, ACI Mater. J. 104 (3) (2007) 233–241.
[45] H. Ma, S. Qian, Z. Zhang, Z. Lin, V.C. Li, Tailoring engineered cementitious composites with local ingredients, Constr. Build. Mater. 101 (2015) 584–595.
[46] A. Delagrave, M. Pigeon, J. Marchand, É. Revertégat, Influence of chloride ions and pH level on the durability of high performance cement pastes (part II), Cem. Concr. Res. 26 (5) (1996) 749–760.
[47] K. Wang, D.E. Nelsen, W.A. Nixon, Damaging effects of deicing chemicals on concrete materials, Cem. Concr. Compos. 28 (2) (2006) 173–188.